

This discussion paper is/has been under review for the journal Atmospheric Chemistry and Physics (ACP). Please refer to the corresponding final paper in ACP if available.

Elemental composition and clustering of α -pinene oxidation products for different oxidation conditions

A. P. Praplan¹, S. Schobesberger¹, F. Bianchi^{2,3}, M. P. Rissanen¹, M. Ehn¹, T. Jokinen¹, H. Junninen¹, A. Adamov¹, A. Amorim⁴, J. Dommen², J. Duplissy⁵, J. Hakala¹, A. Hansel^{6,7}, M. Heinritzi^{8,6}, J. Kangasluoma¹, J. Kirkby^{9,8}, M. Krapf², A. Kürten⁸, K. Lehtipalo¹, F. Riccobono², L. Rondo⁸, N. Sarnela¹, M. Simon⁸, A. Tomé⁴, J. Tröstl², P. M. Winkler¹⁰, C. Williamson⁸, P. Ye¹¹, J. Curtius⁸, U. Baltensperger², N. M. Donahue¹¹, M. Kulmala^{1,5}, and D. R. Worsnop^{1,12}

¹Department of Physics, P.O. Box 64, 00014 University of Helsinki, Finland

²Laboratory of Atmospheric Chemistry, Paul Scherrer Institute, 5232 Villigen PSI, Switzerland

³Institute for Atmospheric and Climate Science, ETH Zurich, 8092 Zurich, Switzerland

⁴Laboratory for Systems, Instrumentation, and Modeling in Science and Technology for Space and the Environment (SIM), University of Lisbon and University of Beira Interior, 1749-016 Lisbon, Portugal

⁵Helsinki Institute of Physics, University of Helsinki, Helsinki, Finland

⁶University of Innsbruck, Institute for Ion Physics and Applied Physics, Technikerstrasse 25, 6020 Innsbruck, Austria

Composition and clustering of α -pinene oxidation products

A. P. Praplan et al.

Title Page

Abstract

Introduction

Conclusions

References

Tables

Figures

◀

▶

◀

▶

Back

Close

Full Screen / Esc

Printer-friendly Version

Interactive Discussion



⁷Ionicon Analytik, Eduard Bodem-Gasse 3, 6020 Innsbruck, Austria

⁸Institute for Atmospheric and Environmental Sciences, Goethe University Frankfurt am Main, Altenhöferallee 1, 60438 Frankfurt am Main, Germany

⁹CERN, CH1211, Geneva, Switzerland

¹⁰Faculty of Physics, University of Vienna, Boltzmanngasse 5, 1090 Wien, Austria

¹¹Center for Atmospheric Particle Studies, Carnegie Mellon University, 5000 Frobes Ave, Pittsburgh, PA 15213, USA

¹²Aerodyne Research Incorporated, Billerica, MA 01821, USA

Received: 7 November 2014 – Accepted: 11 November 2014 – Published: 9 December 2014

Correspondence to: A. P. Praplan (arnaud.praplan@gmail.com)

Published by Copernicus Publications on behalf of the European Geosciences Union.

Composition and
clustering of
 α -pinene oxidation
products

A. P. Praplan et al.

Title Page

Abstract

Introduction

Conclusions

References

Tables

Figures

◀

▶

◀
Back

▶
Close

Full Screen / Esc

Printer-friendly Version

Interactive Discussion



Abstract

This study presents the difference between oxidised organic compounds formed by α -pinene ozonolysis and hydroxyl radical (OH) oxidation in the CLOUD environmental chamber. The results from three Atmospheric Pressure interface Time-Of-Flight (APi-TOF) mass spectrometers measuring simultaneously the composition of naturally charged, as well as neutral species (via chemical ionisation with nitrate) are discussed. Natural chemical ionisation takes place in the CLOUD chamber and organic oxidised compounds form clusters with nitrate, bisulphate, bisulphate/sulphuric acid clusters, ammonium, and dimethylaminium, or get protonated. This process is selective towards various oxidised organic compounds, so that in order to get a comprehensive picture of the elemental composition of oxidation products, several instruments must be used. A comparison between oxidation products containing 10 and 20 carbon atoms is presented. Oxidation products from ozonolysis showed a higher oxidation state than the ones from OH oxidation. Also, highly oxidised organic compounds are shown to be formed in the early stages of the oxidation, for low α -pinene levels.

1 Introduction

Oxidation reactions of organic vapours in the atmosphere and the subsequent condensation of their products is a source of secondary organic aerosol (SOA, see e.g. Kanakidou et al., 2005; Fuzzi et al., 2006; Hallquist et al., 2009 and references therein). Because of the vast number of different compounds in the atmosphere, with various structures and functionalities, detailed oxidation mechanisms are usually insufficiently understood and poorly represented in atmospheric chemical models, especially for larger and complex molecules (Goldstein and Galbally, 2007; Kroll and Seinfeld, 2008). Traditionally, oxidised organic compounds have been considered condensing on small pre-existing particles (few nanometres in diameter) to make them grow up to cloud condensation nuclei sizes (larger than 50 to 100 nm diameter). In general, the more oxidised

Title Page	
Abstract	Introduction
Conclusions	References
Tables	Figures
	
Back	Close
Full Screen / Esc	
Printer-friendly Version	
Interactive Discussion	

dised these products, the lower is their volatility and therefore can condense on smaller particles (Pankow, 1994; Seinfeld and Pankow, 2003; Donahue et al., 2006). However, new studies have shown that α -pinene oxidation products (and organic oxidised compounds in general) do not only participate in particle growth, but also directly influence 5 particle formation rates (Riccobono et al., 2012; Kulmala et al., 2013). It has been shown that sulfuric acid form clusters, which are stabilised by oxidised organic compounds participating directly in the nucleation process (Metzger et al., 2010; Riccobono et al., 2014). Other compounds such as ammonia (Kirkby et al., 2011; Schobesberger et al., 2014) or amines (Almeida et al., 2013; Kürten et al., 2014) can promote sulfuric 10 acid nucleation as well due to an efficient acid-base stabilization mechanism.

Monoterpenes ($C_{10}H_{16}$) are a family of biogenic volatile organic compounds. In boreal forests α -pinene is the most abundant monoterpene. It has been extensively studied in laboratory experiments during the past decades due to its large SOA formation potential (Hoppel et al., 2001; Lee and Kamens, 2005; Eddingsaas et al., 2012a). Two 15 oxidation pathways are known (see Fig. 1):

- Ozonolysis, in which ozone (O_3) reacts with the α -pinene double bond, forming a primary ozonide, which will decompose in Criegee intermediates (Ma et al., 2008; Novelli et al., 2014). These can form carboxylic acids (via rearrangement of dioxiranes) or vinylhydroperoxides that, upon hydroxyl radical (OH) loss, lead to carbonyl compounds.
- OH oxidation, in which the radical adds to the α -pinene double bond (or abstracts an hydrogen atom from α -pinene) resulting in the formation of an alkyl radical. This radical reacts immediately under atmospheric conditions with molecular oxygen (O_2) forming a peroxy radical (RO_2). This peroxy radical can react with various 20 species including other peroxy radicals.

This figure is discussed more extensively in Sect. 3.3. Both gas phase and particulate α -pinene oxidation products were investigated and more detailed chemical analysis became available as analytical methods progressed (Hatakeyama et al., 1989; Ka- 25 30802

[Title Page](#)[Abstract](#)[Introduction](#)[Conclusions](#)[References](#)[Tables](#)[Figures](#)[◀](#)[▶](#)[◀](#)[▶](#)[Back](#)[Close](#)[Full Screen / Esc](#)[Printer-friendly Version](#)[Interactive Discussion](#)

mens et al., 1999; Claeys et al., 2009; Eddingsaas et al., 2012a, b; Winkler et al., 2012). Products such as the dicarboxylic acid *cis*-pinic acid ($C_9H_{14}O_4$, Christoffersen et al., 1998), the tricarboxylic acid 3-methyl-1,2,3-butanetricarboxylic acid (MBTCA, $C_8H_{12}O_6$, Szmigielski et al., 2007) and oligomeric compounds (Tolocka et al., 2004; Müller et al., 2009) were identified. Ehn et al. (2012, 2014) and Schobesberger et al. (2013) have recently observed highly oxidised multifunctional organic compounds (i.e. extremely low volatility organic compounds (ELVOCs), already predicted by Kulmala et al., 1998) in laboratory experiments and in Hyvijärvi, Finland, with oxygen-to-carbon ratios ($O : C$) larger than 1. The more oxidised the compounds the lower their volatility and hence their contribution to SOA (Donahue et al., 2011). As an alternative to $O : C$, Kroll et al. (2011) use the average oxidation state of carbon \overline{OS}_C as a metric for the degree of oxidation of atmospheric organic compounds. It can be estimated by $\overline{OS}_C \approx 2(O : C) - H : C$.

As the formation of newly observed compounds from field studies or from laboratory experiments could not be explained with “traditional” atmospheric chemistry (Atkinson, 2000), new suggestions for mechanisms have been published. Intramolecular reactions seem to play an especially important role in the formation of highly oxidised compounds (Peeters et al., 2001; Vereecken and Peeters, 2004; Ma et al., 2008; Ehn et al., 2014). However, current atmospheric chemical models include only few such non-traditional oxidation mechanisms (e.g. intramolecular reactions).

Building on this knowledge, experiments have been conducted within the CLOUD project at CERN to investigate the formation of new particles from organic vapours under various oxidation regimes (ozone and hydroxyl radical oxidation). The CLOUD chamber (described in more detail in the next section) has extremely low background contamination levels, and therefore provides excellent conditions for unperturbed nucleation experiments (Schnitzhofer et al., 2014). Additionally, CLOUD makes use of CERN’s Proton Synchrotron (PS) facility in order to simulate various galactic cosmic ray (GCR) intensities (increased ion pair concentration).

Composition and clustering of α -pinene oxidation products

A. P. Praplan et al.

[Title Page](#)

[Abstract](#)

[Introduction](#)

[Conclusions](#)

[References](#)

[Tables](#)

[Figures](#)

◀

▶

◀

▶

[Back](#)

[Close](#)

[Full Screen / Esc](#)

[Printer-friendly Version](#)

[Interactive Discussion](#)



The results presented in this manuscript focus on the underlying chemistry of α -pinene oxidation, based on mass spectrometry measurements. The study investigates positive, negative and neutral species present in the CLOUD chamber during α -pinene oxidation at a given relative humidity and temperature. Two different oxidation pathways have been investigated: Ozonolysis in the presence of an OH scavenger and OH oxidation with only background levels of ozone. We first present the general differences between both systems before focussing on a subset of oxidised organic compounds, to show how the elemental composition of oxidation products varies. The interactions of these various compounds with inorganic ions and clusters is discussed and their temporal evolution is presented in order to investigate formation mechanisms.

2 Experimental

The CLOUD (Cosmics Leaving OUtdoor Droplets) facility is located at CERN (Meyrin, Switzerland) and consists of a 26.1 m³ stainless steel reactor in a temperature-controlled enclosure. The facility is described in more detail by Kirkby et al. (2011). Thorough cleaning with ultra pure water and heat (373 K) decreases contaminant levels to a minimum. The chamber is used as a continuously stirred reactor. It is constantly flushed with ultrapure air produced from cryogenic molecular nitrogen (N₂) and oxygen (O₂) in a 79 : 21 ratio. Trace gases are carefully adjusted and monitored. An optical fibre ultra-violet (UV) irradiation setup (Kupc et al., 2011) produces hydroxyl radicals from nitrous acid (HONO) photolysis for the OH oxidation experiments (Cox, 1974). HONO is generated continuously from sodium nitrite and sulphuric acid solutions according to the method described in Taira and Kanda (1990). An additional strong UV source, a factor-100 higher intensity UV-source installed in a quartz tube inserted into the chamber (called “UV sabre”) is used to increase OH levels in the OH experiment presented in this manuscript. Additionally, field cage electrodes situated at the top and bottom of the chamber, respectively, generate an electric field (20 kV m⁻¹) that removes existing ions in less than one second. This enables the investigation of nucleation under

Composition and clustering of α -pinene oxidation products

A. P. Praplan et al.

Title Page

Abstract

Introduction

Conclusions

References

Tables

Figures

◀

▶

◀

▶

Back

Close

Full Screen / Esc

Printer-friendly Version

Interactive Discussion



neutral conditions. The use of a pion beam from CERN's Proton Synchrotron increases the amount of ions present in the chamber. When neither the electrodes nor the beam are used, the ions in the chamber arise from the natural galactic cosmic rays penetrating the chamber.

- 5 The CLOUD7 campaign was conducted between September and December 2012. Table 1 summarises the conditions of representative experiments for ozonolysis and OH oxidation used in this analysis. For the ozonolysis experiment ozone was set to about 22 ppbv and the oxidation was triggered by the injection of α -pinene. For the OH oxidation experiment HONO and α -pinene were introduced until they reached stable concentrations (about 1.9 ± 0.7 ppbv and 1250 pptv, respectively). In this case the oxidation was triggered by turning on the UV lights.
- 10

State of the art particle counters and sizers were deployed, as well as recently developed mass spectrometers. The instrumentation is described in detail in Almeida et al. (2013). We present in this manuscript results from three high-resolution mass

15 spectrometers:

- an Atmospheric Pressure interface Time-Of-Flight (APi-TOF) mass spectrometer in positive mode,
- an APi-TOF mass spectrometer in negative mode (Junninen et al., 2010),
- and a Chemical Ionisation APi-TOF (CI-APi-TOF) using nitrate (NO_3^-) as ionising reagent (Jokinen et al., 2012)

20 Both APi-TOF mass spectrometers measure ions and charged molecular clusters as present in the chamber, whereas the CI-APi-TOF measures neutral molecules and clusters charged by NO_3^- (either by proton transfer or by forming an adduct). High-resolution spectra acquired with these instruments were analysed using the *tofTools* data analysis software (Junninen et al., 2010).

25

[Title Page](#)[Abstract](#)[Introduction](#)[Conclusions](#)[References](#)[Tables](#)[Figures](#)[◀](#)[▶](#)[◀](#)[▶](#)[Back](#)[Close](#)[Full Screen / Esc](#)[Printer-friendly Version](#)[Interactive Discussion](#)

3 Results and discussion

3.1 Mass defect plots

Mass defect plots are a convenient way to visualise high-resolution mass spectral data (Kendrick, 1963; Sleno, 2012). The difference between the exact mass and the integer (nominal) mass of a detected compound (i.e. its mass defect) is plotted against its exact mass.

Figure 2 presents the mass defect plots from three different instruments (positive and negative API-TOFs, as well as nitrate Cl-API-TOF) for the two different oxidation conditions. The mass spectra have been averaged over the time periods when sulfuric acid reached a stable concentration.

All plots show a similar structure, as the signals tend to be organised in “bands”, resembling clouds of markers oriented diagonally (from upper left to lower right). They are the most pronounced in mass defect plots for anions (middle column). The first band is located on the left with lower mass defect values and the following bands are placed more on the right and higher on the mass defect axis. The size of the markers is proportional to the natural logarithm of the peak area in the mass spectra ($> 0.01 \text{ s}^{-1}$ in this study) and they have been coloured according to the retrieved elemental composition (gray points have unidentified composition). The organic compounds in the first band are predominantly species with 10 carbon atoms (“C₁₀”), while in the second band they are mainly compounds with 20 carbon atoms (“C₂₀”), but also compounds with a different number of carbon atoms are detected (“C₈”, “C₉”, “C₁₉”, etc.).

The elemental compositions are not fully unambiguous due to O₆ and SO₄ having nearly identical masses (95.969 and 95.952 amu, respectively), requiring even higher resolution to distinguish between them. Nevertheless, based on previous studies, isotopic patterns, and assumptions on chemical reactions, the elemental composition of most compounds could be retrieved. For signals with low intensity, the elemental composition could sometimes be inferred by extending a pattern (e.g. increas-

[Title Page](#)[Abstract](#)[Introduction](#)[Conclusions](#)[References](#)[Tables](#)[Figures](#)[◀](#)[▶](#)[◀](#)[▶](#)[Back](#)[Close](#)[Full Screen / Esc](#)[Printer-friendly Version](#)[Interactive Discussion](#)

ing or decreasing the number of oxygen atoms or adding sulfuric acid molecules to $(C_{10}H_bO_c)HSO_4^-$.

In the mass defect plots from negative and neutral species the markers in red represent the clusters containing only sulfuric acid molecules ($(H_2SO_4)_nHSO_4^-$ ($n = 1, 2$)) and blue points represent nitric acid clusters ($(HNO_3)_nNO_3^-$ ($n = 1, 2$)). Ammonia-sulfuric acid clusters are present in the negative spectra. They are the points marked in pink with mass-to-charge ratio larger than 400 Th and mass defect smaller than -0.1 (Bianchi et al., 2014). Some compounds are deprotonated (dark green) and, because of the presence of NO_x in the OH oxidation experiment some compounds are organonitrates (bound to NO_3^- , light blue). At higher masses, the bands contain clusters of organic molecules and inorganic ions ($(H_2SO_4)_nHSO_4^-$ ($n = 0, 1, 2$) or NO_3^-). The binding to sulfuric acid clusters ($(H_2SO_4)_nHSO_4^-$ ($n = 1, 2$)) is more pronounced for the ozonolysis-only experiment, even though H_2SO_4 levels are similar in both experiments (within a factor of 2).

Clusters detected in the positive spectra almost exclusively consist of an α -pinene oxidation product and a cation (either a proton (H^+), an ammonium (NH_4^+), or a dimethylaminium ($C_2H_8N^+$)), even for the higher masses. They rarely contain neutral ammonia (NH_3) or dimethylamine (C_2H_7N) molecules. In Fig. 2, no distinction is made between NH_4^+ and $C_2H_8N^+$ containing clusters.

The third band ("C₃₀") is not evident in spectra of anions and the fourth band ("C₄₀") is absent. These have been observed by Schobesberger et al. (2013), though in a different reaction system (OH oxidation of pinanediol, a first generation oxidation product of α -pinene). This suggests that OH oxidation of first generation products of α -pinene ozonolysis is conducive to the binding of H_2SO_4 for the compounds of the third and fourth band in the negative spectra. Nevertheless, "C₃₀" and "C₄₀" bands are seen in spectra of positive clusters in both cases with a weaker signal for the third and fourth bands compared to the first two. However, as none of these bands is observed for the neutral clusters for either oxidation conditions, these large compounds evidently do not form stable clusters with NO_3^- . This means that if large oxidised organic compounds

Composition and clustering of α -pinene oxidation products

A. P. Praplan et al.

[Title Page](#)

[Abstract](#)

[Introduction](#)

[Conclusions](#)

[References](#)

[Tables](#)

[Figures](#)

◀

▶

◀
Back

▶
Close

[Full Screen / Esc](#)

[Printer-friendly Version](#)

[Interactive Discussion](#)



Composition and clustering of α -pinene oxidation products

A. P. Praplan et al.

are formed in the gas phase before being protonated or binding to ions, their functionalities favour binding with NH_4^+ or $\text{C}_2\text{H}_8\text{N}^+$ rather than with NO_3^- or $(\text{H}_2\text{SO}_4)_n\text{HSO}_4^-$ ($n = 0, 1, 2$), pointing towards compounds with acidic (carboxylic) functionalities.

3.2 Average carbon oxidation state, $\overline{\text{OS}}_{\text{C}}$

- 5 The average carbon oxidation state ($\overline{\text{OS}}_{\text{C}}$) of the identified oxidised organic compounds in the clusters for both oxidation conditions is presented in Fig. 3. The results from all three instruments are combined and weighted averages for bands are shown as large gray symbols (“ C_0 ” for $\text{C} < 8$, “ C_{10} ” for $\text{C} = 8\text{--}12$, “ C_{20} ” for $\text{C} = 18\text{--}20$, “ C_{30} ” for $\text{C} = 28\text{--}30$, and “ C_{40} ” for $\text{C} = 38\text{--}40$).
- 10 The $\overline{\text{OS}}_{\text{C}}$ trends are similar for both oxidation conditions. The values for the “ C_0 ” band are high (i.e. compounds are more oxidised) for negative and neutral species but below zero (i.e. compounds are less oxidised) for the positive species. The compounds detected in the neutral channel are slightly more oxidised. These values converge (decreasing for negative and neutral species and increasing for positive species) and are
- 15 about the same for the “ C_{20} ” band. Averaged $\overline{\text{OS}}_{\text{C}}$ for the “ C_{20} ” band is about -0.3 in the ozonolysis-only experiment and about -0.7 in the OH oxidation experiment, independent of which ions the oxidised organic compounds are bound to.

Note that $\overline{\text{OS}}_{\text{C}}$ neglects the effect of peroxide functionalities, which one expects to be abundant for low NO_x levels as it is the case in the ozonolysis-only experiment. Taking this effect into account would lower the averaged $\overline{\text{OS}}_{\text{C}}$ values for this experiment, reducing the difference between the oxidation conditions. The present comparison is biased, though, as it should be performed with experiments at similar NO_x levels, but such data are not available within this study. However, $\overline{\text{OS}}_{\text{C}} \approx 2(\text{O} : \text{C}) - \text{H} : \text{C}$ remains a useful, operationally defined quantity.

25 The next sections focus on the differences in elemental composition and clustering behaviour of newly formed compounds for either oxidation conditions. For the sake

[Title Page](#)

[Abstract](#)

[Introduction](#)

[Conclusions](#)

[References](#)

[Tables](#)

[Figures](#)

◀

▶

[Back](#)

[Close](#)

[Full Screen / Esc](#)

[Printer-friendly Version](#)

[Interactive Discussion](#)



of clarity, only a detailed analysis of clusters containing C₁₀ and C₂₀ oxidised organic compounds is presented.

3.3 Elemental composition of selected oxidised organics

The identified C₁₀ and C₂₀ oxidised organic compounds from the clusters with highest signal were grouped regardless of which inorganic ions they were bound to (Figs. 4 and 5). These stacked bars represent the clusters' peak area in the mass spectra in which the oxidised organic compounds were identified. No quantitative comparison is made. From both overview figures, charged species are discussed first, and later compared to neutral species, comparing both oxidation pathways. In the end, time series of some clusters are presented in order to understand their temporal evolution.

3.3.1 Ions

The differences in compound distribution between pure ozonolysis using OH scavenger (top) and OH oxidation (bottom) for positively (left) and negatively (middle) charged clusters containing a C₁₀ oxidised compound are illustrated in Fig. 4. The range of compounds measured is similar for both experiments, but their distribution patterns differ. For positively charged species elemental compositions C₁₀H₁₂O_{0–3}, C₁₀H₁₄O_{1–7}, and C₁₀H₁₆O_{2–8} have been identified in both experiments, whereas elemental composition C₁₀H₁₈O_{2–9}, for instance, are only seen in the OH oxidation experiment. For the negatively charged species the C₁₀H₁₂O_{5–12}, C₁₀H₁₄O_{2–13} and C₁₀H₁₆O_{6–11} compositions are present in both experiments, whereas compositions C₁₀H₁₆O_{1–5} are typical for OH oxidation. Due to the previously addressed issue with O₆ and SO₄ having very close masses, the attribution in the negative spectra of composition such as (C₁₀H_bO_c)(H₂SO₄)_nHSO₄[–] remains ambiguous as their signal is small and interferes with (C₁₀H_{b+2}O_{c+6})(H₂SO₄)_{n–1}HSO₄[–] ($n = 1, 2$).

The corresponding analysis for the second band (C₂₀ compounds) reveals clear differences between ozonolysis and OH oxidation in the formation of ion clusters (Fig. 5).

Title Page

Abstract

Introduction

Conclusions

References

Tables

Figures

◀

▶

Back

Close

Full Screen / Esc

Printer-friendly Version

Interactive Discussion



Composition and clustering of α -pinene oxidation products

A. P. Praplan et al.

[Title Page](#)

[Abstract](#)

[Introduction](#)

[Conclusions](#)

[References](#)

[Tables](#)

[Figures](#)

[◀](#)

[▶](#)

[◀](#)
[▶](#)

[◀](#)
[▶](#)

[Back](#)

[Close](#)

[Full Screen / Esc](#)

[Printer-friendly Version](#)

[Interactive Discussion](#)



((E)LVOCs). In our experiments, NO_x is only relevant for the OH oxidation pathway. No explicit structure is given for products of intramolecular H-abstraction, as it is yet unknown, which H atom would be abstracted first. Termination reaction branching ratios leading to the various functionalities are influenced by HO_2 , RO_2 and NO_x levels.

Therefore, there is a minor difference in functional groups for species with a lower number of oxygen atoms: ozonolysis favours carbonyl functional groups (ketones, aldehydes), while OH oxidation produces hydroxyl (alcohols) functionalities (Atkinson, 2000; Vereecken et al., 2012; Taatjes et al., 2013). However, for multifunctional species (more than 5 oxygen atoms, ELVOCs), no particular functional group is dominant.

Bipolar charging probabilities determined for aerosol particles are sometimes extrapolated down to 1 nm diameters (e.g. Jiang et al., 2011) ignoring the role of chemical composition. Although the present results do not necessarily apply to all types of clusters, they do suggest that this extrapolation is valid down to around 1.5 nm in mobility diameter, which is roughly the size of the detected C_{20} containing clusters (Ehn et al., 2011). Below this size, compounds clearly behave differently depending on polarity and charger ion composition.

Ehn et al. (2012) identified $\text{C}_{10}\text{H}_{14}\text{O}_{7-11,13}$, $\text{C}_{10}\text{H}_{16}\text{O}_{7-11}$, $\text{C}_{20}\text{H}_{30}\text{O}_{12-16,18}$, and $\text{C}_{20}\text{H}_{32}\text{O}_{11,13,15}$ in α -pinene ozonolysis chamber experiments (and a subset of these in the boreal forest site in Hytylä, Finland). All of these, were also identified during our study in either experiment.

3.3.2 Neutral species

The clusters containing C_{10} and C_{20} oxidised compounds from the ozonolysis only experiment (top) and the OH oxidation (bottom), respectively, is depicted in the right columns of Figs. 4 and 5.

$\text{C}_{10}\text{H}_{15}\text{O}_{8,10}$ (bound to NO_3^-) are seen in the neutral spectra of the OH oxidation experiment (Fig. 4, bottom right). They are also seen in the negative spectra (bottom middle).

Comparing the mass spectra of the neutral species with the previously discussed plots from the negative clusters, it appears that the natural ionisation happening in the chamber with HSO_4^- is less selective than the chemical ionisation with NO_3^- in the CI-APi-TOF ion source. Therefore, not all the neutral species appear in the spectra of the neutral clusters. The detected compounds represent ELVOCs though and were shown to be proportional to the (total) amount of oxidised compounds (Ehn et al., 2014). Therefore, for a comprehensive detection of α -pinene oxidation products and their mechanistic interpretation, HSO_4^- seems to perform better than NO_3^- as an ionisation reagent.

Schobesberger et al. (2013) presents a similar analysis for oxidation reactions of pinanediol with OH (and high H_2SO_4 levels). No CI-APi-TOF was used for those experiments and the authors claim that the composition of neutral clusters is similar to that of negatively charged clusters. Even though this statement may be true, it cannot be shown with only one type of chemical ionisation.

While the distribution of clusters in the neutral spectra compared to the positive and negative spectra is different for C_{10} compounds, it is almost identical for the C_{20} compounds. Therefore, C_{20} compounds independently of their formation pathways display a similar reactivity towards NH_4^+ , $\text{C}_2\text{H}_8\text{N}^+$, HSO_4^- and NO_3^- , even though the distribution is shifted towards slightly more oxidised compounds in the neutral spectra, especially for $\text{C}_{20}\text{H}_{30,32}\text{O}_c$. In our experiments, the negative spectra is sensitive to a broader range of O : C, in particular for $\text{C}_{20}\text{H}_{30}\text{O}_c$.

4 Clusters time series

Normalised time series have been derived for all three instruments to investigate formation mechanisms. The time series varies from 1 min (positive data) to 5 min (negative OH oxidation data). The other time series have a 2 min time resolution. These have been set in order to optimise the signal-to-noise ratio in each of the spectra.

[Title Page](#)[Abstract](#)[Introduction](#)[Conclusions](#)[References](#)[Tables](#)[Figures](#)[◀](#)[▶](#)[◀](#)[▶](#)[Back](#)[Close](#)[Full Screen / Esc](#)[Printer-friendly Version](#)[Interactive Discussion](#)

Analysis of positive C₂₀ containing clusters in the ozonolysis experiment shows that most oxidised compounds (up to O₁₈, not shown) appear almost immediately after the beginning of the experiment (vertical black line) and reach their maximum concentration the earliest (Fig. 6). This is observed for clusters of C₂₀H₃₀O_c with either NH₄⁺ or C₂H₈N⁺. The signals of the clusters containing the most oxidised compounds decrease after reaching their maximum, whereas the signals of the other clusters level off. This corresponds to the mixing ratio of α -pinene slowly reaching its equilibrium concentration towards the end of the run, stabilizing the oxidation conditions. This indicates that when α -pinene is very low, fewer termination reactions (with RO₂) happen, allowing further oxidation by successive intramolecular H-shifts as suggested by Ehn et al. (2014), see Fig. 1. This observation is in line with smog chamber experiments (Pfaffenberger et al., 2013), showing that higher O : C of SOA is achieved with low α -pinene levels. This result contrasts with the view that the most oxidised organic compounds are formed only after long oxidants exposure time. Highly oxidised organic compounds can also be formed very quickly, depending on the oxidation conditions.

For the OH oxidation experiment the α -pinene concentration is high from the beginning of the run and OH is produced from HONO photolysis by UV light. In this case the signals for the presented positive clusters containing C₂₀H₃₂O_c (with either NH₄⁺ or C₂H₈N⁺) rise almost simultaneously, so that no similar conclusion can be drawn, even at 1 min time resolution. Trying to increase the time resolution to observe which signals increase first would lead to a too low signal-to-noise ratio. A similar (but less clear) trend is observed as well in neutral spectra (Fig. 7).

The analysis of time series for the negative spectra is not straightforward, due to the lower signal and isobaric species. Nevertheless, Fig. 8 shows the time series for selected clusters containing C₂₀H₃₀O_c species for the ozonolysis-only experiment and containing C₂₀H₂₈O_c species for the OH oxidation experiments. The data show that, in the ozonolysis-only experiment, the clusters with an additional neutral sulfuric acid molecule are formed later. Therefore, the mechanism suggested earlier as Eq. (3) is the most likely to happen. It remains unclear, though, if the cluster contains one covalently

[Title Page](#)[Abstract](#)[Introduction](#)[Conclusions](#)[References](#)[Tables](#)[Figures](#)[◀](#)[▶](#)[◀](#)[▶](#)[Back](#)[Close](#)[Full Screen / Esc](#)[Printer-friendly Version](#)[Interactive Discussion](#)

bound C₂₀ oxidised compound or two C₁₀ compounds. The slight decrease of averaged OS_C from the “C₁₀” to the “C₂₀” band discussed earlier suggests that two C₁₀ peroxy radicals probably react together (losing oxygen atoms) before binding to HSO₄⁻.

5 Conclusions

- Oxidation of α -pinene was conducted in the CLOUD chamber. The simultaneous use of three different mass spectrometers provides a unique insight of the chemical reaction mechanisms happening in the early stage of α -pinene oxidation and molecular cluster formation.

Charged clusters consist of oxidised organic compounds binding to a core ion (bisulfate or nitrate for negative clusters and hydronium, ammonium, or aminium for positive clusters). Molecular clusters including additional sulfuric acid molecules have also been detected in the negative spectra for ozonolysis, while in the positive spectra, even clusters with high masses rarely contain neutral ammonia or dimethylamine molecules. The results show the selectivity of this chemical ionisation process. Especially the difference between ionisation with NO₃⁻ and HSO₄⁻ can be seen from the broader range of C₁₀ oxidised compounds observed in the negative spectra compared to the neutral one. The cluster distribution of the C₂₀ is very similar for all instruments, showing that due to the many functional groups of these species, their affinities towards the various ions present is similar. This also implies that for the analysis of atmospheric clusters containing oxidised organic clusters, the combination of API-TOF and CI-API-TOF mass spectrometers with varying ionisation reagent is important in order to capture a comprehensive picture of formed products, in particular for low molar mass products. Heavier oxidised organic compounds (C₂₀), due to their many functional groups can be similarly charged by various ions, suggesting that the ionisation starts to be independent of the charging mechanism. Even if both oxidation mechanisms differ in their first step, they both lead to the formation of peroxy radicals, which produce multifunctional oxidised organic compounds. For compounds containing a low number of oxygen

Title Page	
Abstract	Introduction
Conclusions	References
Tables	Figures
	
	
Full Screen / Esc	
Printer-friendly Version	
Interactive Discussion	



atoms, ozonolysis products tend to possess more carbonyl functionalities while OH oxidation products have more hydroxyl functionalities and preferentially get protonated or form clusters with cations. However, there is no clear functional group distribution for the compounds with a larger degree of oxidation. Their functionalities depend on the termination reactions with HO_2 , RO_2 , or NO_x and bind with cations as well as with anions.

Other differences could be highlighted between the oxidised organic compounds from ozonolysis and OH oxidation besides their clustering behaviour. For instance, the mean carbon oxidation state ($\overline{\text{OS}}_{\text{C}}$) of the oxidised compounds in the clusters when averaged by bands is higher for ozonolysis than for OH oxidation experiment. This difference is due to NO_x present in the OH oxidation experiment only, though.

Time series of the signal of selected clusters indicate that early steps of ozonolysis lead to the formation of highly oxidised compounds. This is due to the low RO_2 concentrations, resulting from low α -pinene levels. This allows RO_2 to react intramolecularly (by H abstractions followed by reaction with O_2) several times before they react with another RO_2 to form stable C_{10} or C_{20} oxidation products. Therefore their O : C is higher. There is consequently no oxidation pathway from low to highly oxidised molecules, but rather a branching of oxidation levels according to oxidation conditions. Negative clusters time series show that $(\text{C}_{20}\text{H}_{30}\text{O}_{\text{c}})(\text{H}_2\text{SO}_4)\text{HSO}_4^-$ clusters are formed in the ozonolysis experiment later than $(\text{C}_{20}\text{H}_{30}\text{O}_{\text{c}})\text{HSO}_4^-$. Nevertheless, it remains unclear if the $(\text{C}_{20}\text{H}_{30}\text{O}_{\text{c}})\text{HSO}_4^-$ consist of covalently bound C_{20} oxidised compounds or of two C_{10} compounds. The slight decrease of averaged $\overline{\text{OS}}_{\text{C}}$ from the “ C_{10} ” to “ C_{20} ” band for negative clusters suggests that C_{20} molecules are formed upon loss of O_2 from two C_{10} peroxy radicals before binding to an ion. Due to the time resolution limitations it was not possible to draw similar conclusions for the OH oxidation experiment.

Finally, the results presented are limited to the used oxidation conditions in our experiments. Broader ranges of temperatures, relative humidities, NO_x and α -pinene levels need to be investigated to enable generalisation of the conclusions of the present study and refine clustering mechanisms of oxidised organic compounds.

[Title Page](#)[Abstract](#)[Introduction](#)[Conclusions](#)[References](#)[Tables](#)[Figures](#)[◀](#)[▶](#)[◀](#)
[Back](#)[▶](#)
[Close](#)[Full Screen / Esc](#)[Printer-friendly Version](#)[Interactive Discussion](#)

Acknowledgements. We would like to thank CERN for supporting CLOUD with important technical and financial resources, and for providing a particle beam from the CERN Proton Synchrotron. We also thank P. Carrie, L.-P. De Menezes, J. Dumollard, K. Ivanova, F. Josa, I. Krasin, R. Kristic, A. Laassiri, O. S. Maksumov, B. Marichy, H. Martinati, S. V. Mizin, R. Sitals, A. Wasem and M. Wilhelmsson for their important contributions to the experiment. This research has received funding from the EC Seventh Framework Programme (Marie Curie Initial Training Network “CLOUD-ITN” no. 215072, MC-ITN “CLOUD-TRAIN” no. 316662, ERC-Starting “MOCA-PAF” grant no. 57360 and ERC-Advanced “ATMNUCLE” grant no. 227463), PEGASOS project funded by the European Commission under the Framework Programme 7 (FP7-ENV-2010-265148), the German Federal Ministry of Education and Research (project nos. 01LK0902A and 01LK1222A), the Swiss National Science Foundation (project nos. 200020_135307 and 206620_141278), the Academy of Finland (Center of Excellence project no. 1118615), the Academy of Finland (135054, 133872, 251427, 139656, 139995, 137749, 141217, 141451), the Finnish Funding Agency for Technology and Innovation, the Väisälä Foundation, the Nessling Foundation, the Austrian Science Fund (FWF; project no. J3198-N21), the Portuguese Foundation for Science and Technology (project no. CERN/FP/116387/2010), the Swedish Research Council, Vetenskapsrådet (grant 2011-5120), the Presidium of the Russian Academy of Sciences and Russian Foundation for Basic Research (grants 08-02-91006-CERN and 12-02-91522-CERN), the U.S. National Science Foundation (grants AGS1136479 and CHE1012293), and the Davidow Foundation. We thank the tofTools team for providing tools for mass spectrometry analysis.

References

- Almeida, J., Schobesberger, S., Kürten, A., Ortega, I. K., Kupiainen-Määttä, O., Praplan, A. P., Adamov, A., Amorim, A., Bianchi, F., Breitenlechner, M., David, A., Dommen, J., Donahue, N. M., Downard, A., Dunne, E., Duplissy, J., Ehrhart, S., Flagan, R. C., Franchin, A., Guida, R., Hakala, J., Hansel, A., Heinritzi, M., Henschel, H., Jokinen, T., Junninen, H., Kajos, M., Kangasluoma, J., Keskinen, H., Kupc, A., Kurtén, T., Kvashin, A. N., Laaksonen, A., Lehtipalo, K., Leiminger, M., Leppä, J., Loukonen, V., Makhmutov, V., Mathot, S., McGrath, M. J., Nieminen, T., Olenius, T., Onnela, A., Petäjä, T., Riccobono, F., Riipinen, I., Rissanen, M., Rondo, L., Ruuskanen, T., Santos, F. D., Sarnela, N., Schallhart, S.,

[Title Page](#)[Abstract](#)[Introduction](#)[Conclusions](#)[References](#)[Tables](#)[Figures](#)[◀](#)[▶](#)[◀](#)[▶](#)[Back](#)[Close](#)[Full Screen / Esc](#)[Printer-friendly Version](#)[Interactive Discussion](#)

Composition and clustering of α -pinene oxidation products

A. P. Praplan et al.

[Title Page](#)

[Abstract](#)

[Introduction](#)

[Conclusions](#)

[References](#)

[Tables](#)

[Figures](#)

◀

▶

◀

▶

[Back](#)

[Close](#)

[Full Screen / Esc](#)

[Printer-friendly Version](#)

[Interactive Discussion](#)



Schnitzhofer, R., Seinfeld, J. H., Simon, M., Sipilä, M., Stozhkov, Y., Stratmann, F., Tomé, A., Tröstl, J., Tsagkogeorgas, G., Vaattovaara, P., Viisanen, Y., Virtanen, A., Vrtala, A., Wagner, P. E., Weingartner, E., Wex, H., Williamson, C., Wimmer, D., Ye, P., Yli-Juuti, T., Carslaw, K. S., Kulmala, M., Curtius, J., Baltensperger, U., Worsnop, D. R., Vehkamäki, H., and Kirkby, J.: Molecular understanding of sulphuric acid–amine particle nucleation in the atmosphere, *Nature*, 502, 359–363, doi:10.1038/nature12663, 2013. 30802, 30805

Atkinson, R.: Atmospheric chemistry of VOCs and NO_x, *Atmos. Environ.*, 34, 2063–2101, doi:10.1016/S1352-2310(99)00460-4, 2000. 30803, 30811

Bianchi, F., Praplan, A. P., Sarnela, N., Dommen, J., Kürten, A., Ortega, I. K., Schobesberger, S., Junninen, H., Simon, M., Tröstl, J., Jokinen, T., Sipilä, M., Adamov, A., Amorim, A., Almeida, J., Breitenlechner, M., Duplissy, J., Ehrhart, S., Flagan, R. C., Franchin, A., Hakala, J., Hansel, A., Heinritzi, M., Kangasluoma, J., Keskinen, H., Kim, J., Kirkby, J., Laaksonen, A., Lawler, M. J., Lehtipalo, K., Leiminger, M., Makhmutov, V., Mathot, S., Onnela, A., Petäjä, T., Riccobono, F., Rissanen, M. P., Rondo, L., Tomé, A., Virtanen, A., Viisanen, Y., Williamson, C., Wimmer, D., Winkler, P. M., Ye, P., Curtius, J., Kulmala, M., Worsnop, D. R., Donahue, N. M., and Baltensperger, U.: Insight into acid-base nucleation experiments by comparison of the chemical composition of positive, negative, and neutral clusters, *Environ. Sci. Technol.*, 48, 13675–13684, doi:10.1021/es502380b, 2014. 30807

Christoffersen, T., Hjorth, J., Horie, O., Jensen, N., Kotzias, D., Molander, L., Neeb, P., Ruppert, L., Winterhalter, R., Virkkula, A., Wirtz, K., and Larsen, B.: *cis*-Pinic acid, a possible precursor for organic aerosol formation from ozonolysis of α -pinene, *Atmos. Environ.*, 32, 1657–1661, doi:10.1016/S1352-2310(97)00448-2, 1998. 30803

Claeys, M., Iinuma, Y., Szmigielski, R., Surratt, J. D., Blockhuys, F., Van Alsenoy, C., Böge, O., Sierau, B., Gómez-González, Y., Vermeylen, R., Van der Veken, P., Shahgholi, M., Chan, A. W. H., Herrmann, H., Seinfeld, J. H., and Maenhaut, W.: Terpenylic acid and related compounds from the oxidation of α -Pinene: implications for new particle formation and growth above forests, *Environ. Sci. Technol.*, 43, 6976–6982, doi:10.1021/es9007596, 2009. 30803

Cox, R. A.: The photolysis of gaseous nitrous acid, *J. Photochem.*, 3, 175–188, doi:10.1016/0047-2670(74)80018-3, 1974. 30804

Donahue, N. M., Robinson, A. L., Stanier, C. O., and Pandis, S. N.: Coupled partitioning, di-lution, and chemical aging of semivolatile organics, *Environ. Sci. Technol.*, 40, 2635–2643, doi:10.1021/es052297c, 2006. 30802

Composition and clustering of α -pinene oxidation products

A. P. Praplan et al.

[Title Page](#)[Abstract](#)[Introduction](#)[Conclusions](#)[References](#)[Tables](#)[Figures](#)[◀](#)[▶](#)[◀](#)[▶](#)[Back](#)[Close](#)[Full Screen / Esc](#)[Printer-friendly Version](#)[Interactive Discussion](#)

Donahue, N. M., Epstein, S. A., Pandis, S. N., and Robinson, A. L.: A two-dimensional volatility basis set: 1. organic-aerosol mixing thermodynamics, *Atmos. Chem. Phys.*, 11, 3303–3318, doi:10.5194/acp-11-3303-2011, 2011. 30803

Eddingsaas, N. C., Loza, C. L., Yee, L. D., Chan, M., Schilling, K. A., Chhabra, P. S., Seinfeld, J. H., and Wennberg, P. O.: α -pinene photooxidation under controlled chemical conditions – Part 2: SOA yield and composition in low- and high- NO_x environments, *Atmos. Chem. Phys.*, 12, 7413–7427, doi:10.5194/acp-12-7413-2012, 2012a. 30802, 30803

Eddingsaas, N. C., Loza, C. L., Yee, L. D., Seinfeld, J. H., and Wennberg, P. O.: α -pinene photooxidation under controlled chemical conditions – Part 1: Gas-phase composition in low- and high- NO_x environments, *Atmos. Chem. Phys.*, 12, 6489–6504, doi:10.5194/acp-12-6489-2012, 2012b. 30803

Ehn, M., Junninen, H., Schobesberger, S., Manninen, H. E., Franchin, A., Sipilä, M., Petäjä, T., Kerminen, V.-M., Tammet, H., Mirme, A., Mirme, S., Hörrak, U., Kulmala, M., and Worsnop, D. R.: An instrumental comparison of mobility and mass measurements of atmospheric small ions, *Aerosol Sci. Tech.*, 45, 522–532, doi:10.1080/02786826.2010.547890, 2011. 30811

Ehn, M., Kleist, E., Junninen, H., Petäjä, T., Lönn, G., Schobesberger, S., Dal Maso, M., Trimborn, A., Kulmala, M., Worsnop, D. R., Wahner, A., Wildt, J., and Mentel, Th. F.: Gas phase formation of extremely oxidized pinene reaction products in chamber and ambient air, *Atmos. Chem. Phys.*, 12, 5113–5127, doi:10.5194/acp-12-5113-2012, 2012. 30803, 30811

Ehn, M., Thornton, J. A., Kleist, E., Sipilä, M., Junninen, H., Pullinen, I., Springer, M., Rubach, F., Tillmann, R., Lee, B., Lopez-Hilfiker, F., Andres, S., Acir, I.-H., Rissanen, M., Jokinen, T., Schobesberger, S., Kangasluoma, J., Kontkanen, J., Nieminen, T., Kurtén, T., Nielsen, L. B., Jørgensen, S., Kjaergaard, H. G., Canagaratna, M., Maso, M. D., Berndt, T., Petäjä, T., Wahner, A., Kerminen, V.-M., Kulmala, M., Worsnop, D. R., Wildt, J., and Mentel, T. F.: A large source of low-volatility secondary organic aerosol, *Nature*, 506, 476–479, doi:10.1038/nature13032, 2014. 30803, 30812, 30813

Fuzzi, S., Andreae, M. O., Huebert, B. J., Kulmala, M., Bond, T. C., Boy, M., Doherty, S. J., Guenther, A., Kanakidou, M., Kawamura, K., Kerminen, V.-M., Lohmann, U., Russell, L. M., and Pöschl, U.: Critical assessment of the current state of scientific knowledge, terminology, and research needs concerning the role of organic aerosols in the atmosphere, climate, and global change, *Atmos. Chem. Phys.*, 6, 2017–2038, doi:10.5194/acp-6-2017-2006, 2006. 30801

- Goldstein, A. H. and Galbally, I. E.: Known and unexplored organic constituents in the Earth's atmosphere, *Environ. Sci. Technol.*, 41, 1514–1521, doi:10.1021/es072476p, 2007. 30801
- Hallquist, M., Wenger, J. C., Baltensperger, U., Rudich, Y., Simpson, D., Claeys, M., Dommen, J., Donahue, N. M., George, C., Goldstein, A. H., Hamilton, J. F., Herrmann, H., Hoffmann, T., Iinuma, Y., Jang, M., Jenkin, M. E., Jimenez, J. L., Kiendler-Scharr, A., Maenhaut, W., McFiggans, G., Mentel, Th. F., Monod, A., Prévôt, A. S. H., Seinfeld, J. H., Suratt, J. D., Szmigielski, R., and Wildt, J.: The formation, properties and impact of secondary organic aerosol: current and emerging issues, *Atmos. Chem. Phys.*, 9, 5155–5236, doi:10.5194/acp-9-5155-2009, 2009. 30801
- Hatakeyama, S., Izumi, K., Fukuyama, T., and Akimoto, H.: Reactions of ozone with alpha-pinene and beta-pinene in air: yields of gaseous and particulate products, *J. Geophys. Res.*, 94, 13013–13024, doi:10.1029/JD094iD10p13013, 1989. 30802
- Hoppel, W., Fitzgerald, J., Frick, G., Caffrey, P., Pasternack, L., Hegg, D., Gao, S., Leaitch, R., Shantz, N., Cantrell, C., Albrechtinski, T., Ambrusko, J., and Sullivan, W.: Particle formation and growth from ozonolysis of α -pinene, *J. Geophys. Res.*, 106, 27603–27,618, doi:10.1029/2001JD900018, 2001. 30802
- Jiang, J., Chen, M., Kuang, C., Attoufi, M., and McMurry, P. H.: Electrical mobility spectrometer using a diethylene glycol condensation particle counter for measurement of aerosol size distributions down to 1 nm, *Aerosol Sci. Tech.*, 45, 510–521, doi:10.1080/02786826.2010.547538, 2011. 30811
- Jokinen, T., Sipilä, M., Junninen, H., Ehn, M., Lönn, G., Hakala, J., Petäjä, T., Mauldin III, R. L., Kulmala, M., and Worsnop, D. R.: Atmospheric sulphuric acid and neutral cluster measurements using CI-APi-TOF, *Atmos. Chem. Phys.*, 12, 4117–4125, doi:10.5194/acp-12-4117-2012, 2012. 30805
- Junninen, H., Ehn, M., Petäjä, T., Luosujärvi, L., Kotiaho, T., Kostiainen, R., Rohner, U., Gonin, M., Fuhrer, K., Kulmala, M., and Worsnop, D. R.: A high-resolution mass spectrometer to measure atmospheric ion composition, *Atmos. Meas. Tech.*, 3, 1039–1053, doi:10.5194/amt-3-1039-2010, 2010. 30805
- Kamens, R., Jang, M., Chien, C.-J., and Leach, K.: Aerosol formation from the reaction of α -pinene and ozone using a gas-phase kinetics-aerosol partitioning model, *Environ. Sci. Technol.*, 33, 1430–1438, doi:10.1021/es980725r, 1999. 30802
- Kanakidou, M., Seinfeld, J. H., Pandis, S. N., Barnes, I., Dentener, F. J., Facchini, M. C., Van Dingenen, R., Ervens, B., Nenes, A., Nielsen, C. J., Swietlicki, E., Putaud, J. P., Balkan-

Composition and clustering of α -pinene oxidation products

A. P. Praplan et al.

[Title Page](#)

[Abstract](#)

[Introduction](#)

[Conclusions](#)

[References](#)

[Tables](#)

[Figures](#)

◀

▶

◀

▶

[Back](#)

[Close](#)

[Full Screen / Esc](#)

[Printer-friendly Version](#)

[Interactive Discussion](#)



Composition and clustering of α -pinene oxidation products

A. P. Praplan et al.

[Title Page](#)

[Abstract](#)

[Introduction](#)

[Conclusions](#)

[References](#)

[Tables](#)

[Figures](#)



[Full Screen / Esc](#)

[Printer-friendly Version](#)

[Interactive Discussion](#)



Worsnop, D. R.: Direct observations of atmospheric aerosol nucleation, *Science*, 339, 943–946, doi:10.1126/science.1227385, 2013. 30802

Kupc, A., Amorim, A., Curtius, J., Danielczok, A., Duplissy, J., Ehrhart, S., Walther, H., Ickes, L., Kirkby, J., Kürten, A., Lima, J., Mathot, S., Minginette, P., Onnella, A., Rondo, L., and Wagner, P.: A fibre-optic UV system for H_2SO_4 production in aerosol chambers causing minimal thermal effects, *J. Aerosol Sci.*, 42, 532–543, doi:10.1016/j.jaerosci.2011.05.001, 2011. 30804

Kürten, A., Jokinen, T., Simon, M., Sipilä, M., Sarnela, N., Junninen, H., Adamov, A., Almeida, J., Amorim, A., Bianchi, F., Breitenlechner, M., Dommen, J., Donahue, N. M., Duplissy, J., Ehrhart, S., Flagan, R. C., Franchin, A., Hakala, J., Hansel, A., Heinritzi, M., Hutterli, M., Kangasluoma, J., Kirkby, J., Laaksonen, A., Lehtipalo, K., Leiminger, M., Makhmutov, V., Mathot, S., Onnella, A., Petäjä, T., Praplan, A. P., Riccobono, F., Rissanen, M. P., Rondo, L., Schobesberger, S., Seinfeld, J. H., Steiner, G., Tomé, A., Tröstl, J., Winkler, P. M., Williamson, C., Wimmer, D., Ye, P., Baltensperger, U., Carslaw, K. S., Kulmala, M., Worsnop, D. R., and Curtius, J.: Neutral molecular cluster formation of sulfuric acid-dimethylamine observed in real time under atmospheric conditions, *P. Natl. Acad. Sci. USA*, 111, 15019–15024, doi:10.1073/pnas.1404853111, 2014. 30802

Lee, S. and Kamens, R. M.: Particle nucleation from the reaction of α -pinene and O_3 , *Atmos. Environ.*, 39, 6822–6832, doi:10.1016/j.atmosenv.2005.07.062, 2005. 30802

Ma, Y., Russell, A. T., and Marston, G.: Mechanisms for the formation of secondary organic aerosol components from the gas-phase ozonolysis of α -pinene, *Phys. Chem. Chem. Phys.*, 10, 4294–4312, doi:10.1039/B803283A, 2008. 30802, 30803

Metzger, A., Verheggen, B., Dommen, J., Duplissy, J., Prevot, A. S. H., Weingartner, E., Riipinen, I., Kulmala, M., Spracklen, D. V., Carslaw, K. S., and Baltensperger, U.: Evidence for the role of organics in aerosol particle formation under atmospheric conditions, *P. Natl. Acad. Sci. USA*, 107, 6646–6651, doi:10.1073/pnas.0911330107, 2010. 30802

Müller, L., Reinnig, M.-C., Hayen, H., and Hoffmann, T.: Characterization of oligomeric compounds in secondary organic aerosol using liquid chromatography coupled to electrospray ionization Fourier transform ion cyclotron resonance mass spectrometry, *Rapid Commun. Mass Sp.*, 23, 971–979, doi:10.1002/rcm.3957, 2009. 30803

Novelli, A., Vereecken, L., Lelieveld, J., and Harder, H.: Direct observation of OH formation from stabilised Criegee intermediates, *Phys. Chem. Chem. Phys.*, 16, 19941, doi:10.1039/C4CP02719A, 2014. 30802

Composition and clustering of α -pinene oxidation products

A. P. Praplan et al.

Title Page

Abstract

Introduction

Conclusions

References

Tables

Figures

◀

▶

◀
Back

▶
Close

Full Screen / Esc

Printer-friendly Version

Interactive Discussion



Composition and clustering of α -pinene oxidation products

A. P. Praplan et al.

Pankow, J. F.: An absorption model of the gas/aerosol partitioning involved in the formation of secondary organic aerosol, *Atmos. Environ.*, 28, 189–193, doi:10.1016/1352-2310(94)90094-9, 1994. 30802

Peeters, J., Vereecken, L., and Fantechi, G.: The detailed mechanism of the OH-initiated atmospheric oxidation of α -pinene: a theoretical study, *Phys. Chem. Chem. Phys.*, 3, 5489–5504, doi:10.1039/B106555F, 2001. 30803

5 Pfaffenberger, L., Barnet, P., Slowik, J. G., Praplan, A. P., Dommen, J., Prévôt, A. S. H., and Baltensperger, U.: The link between organic aerosol mass loading and degree of oxygenation: an α -pinene photooxidation study, *Atmos. Chem. Phys.*, 13, 6493–6506, doi:10.5194/acp-13-6493-2013, 2013. 30813

10 Riccobono, F., Rondo, L., Sipilä, M., Barnet, P., Curtius, J., Dommen, J., Ehn, M., Ehrhart, S., Kulmala, M., Kürten, A., Mikkilä, J., Paasonen, P., Petäjä, T., Weingartner, E., and Baltensperger, U.: Contribution of sulfuric acid and oxidized organic compounds to particle formation and growth, *Atmos. Chem. Phys.*, 12, 9427–9439, doi:10.5194/acp-12-9427-2012, 2012. 30802

15 Riccobono, F., Schobesberger, S., Scott, C. E., Dommen, J., Ortega, I. K., Rondo, L., Almeida, J., Amorim, A., Bianchi, F., Breitenlechner, M., David, A., Downard, A., Dunne, E. M., Duplissy, J., Ehrhart, S., Flagan, R. C., Franchin, A., Hansel, A., Junninen, H., Kajos, M., Keskinen, H., Kupc, A., Kürten, A., Kvashin, A. N., Laaksonen, A., Lehtipalo, K., Makhmutov, V., Mathot, S., Nieminen, T., Onnela, A., Petäjä, T., Praplan, A. P., Santos, F. D., Schallhart, S., Seinfeld, J. H., Sipilä, M., Spracklen, D. V., Stozhkov, Y., Stratmann, F., Tomé, A., Tsagkogeorgas, G., Vaattovaara, P., Viisanen, Y., Vrtala, A., Wagner, P. E., Weingartner, E., Wex, H., Wimmer, D., Carslaw, K. S., Curtius, J., Donahue, N. M., Kirkby, J., Kulmala, M., Worsnop, D. R., and Baltensperger, U.: Oxidation products of biogenic emissions contribute to nucleation of atmospheric particles, *Science*, 344, 717–721, doi:10.1126/science.1243527, 2014. 30802

20 Schnitzhofer, R., Metzger, A., Breitenlechner, M., Jud, W., Heinritzi, M., De Menezes, L.-P., Duplissy, J., Guida, R., Haider, S., Kirkby, J., Mathot, S., Minginette, P., Onnela, A., Walther, H., Wasem, A., Hansel, A., and the CLOUD Team: Characterisation of organic contaminants in the CLOUD chamber at CERN, *Atmos. Meas. Tech.*, 7, 2159–2168, doi:10.5194/amt-7-2159-2014, 2014. 30803

25 Schobesberger, S., Junninen, H., Bianchi, F., Lönn, G., Ehn, M., Lehtipalo, K., Dommen, J., Ehrhart, S., Ortega, I. K., Franchin, A., Nieminen, T., Riccobono, F., Hutterli, M., Du-

[Title Page](#)

[Abstract](#)

[Introduction](#)

[Conclusions](#)

[References](#)

[Tables](#)

[Figures](#)



[Back](#)

[Close](#)

[Full Screen / Esc](#)

[Printer-friendly Version](#)

[Interactive Discussion](#)



plissy, J., Almeida, J., Amorim, A., Breitenlechner, M., Downard, A. J., Dunne, E. M., Flanagan, R. C., Kajos, M., Keskinen, H., Kirkby, J., Kupc, A., Kürten, A., Kurtén, T., Laaksonen, A., Mathot, S., Onnela, A., Praplan, A. P., Rondo, L., Santos, F. D., Schallhart, S., Schnitzhofer, R., Sipilä, M., Tomé, A., Tsagkogeorgas, G., Vehkamäki, H., Wimmer, D., Baltensperger, U., Carslaw, K. S., Curtius, J., Hansel, A., Petäjä, T., Kulmala, M., Donahue, N. M., and Worsnop, D. R.: Molecular understanding of atmospheric particle formation from sulfuric acid and large oxidized organic molecules, *P. Natl. Acad. Sci. USA*, 110, 17223–17228, doi:10.1073/pnas.1306973110, 2013. 30803, 30807, 30812

Schobesberger, S., Franchin, A., Bianchi, F., Rondo, L., Duplissy, J., Kürten, A., Ortega, I. K., Metzger, A., Schnitzhofer, R., Almeida, J., Amorim, A., Dommen, J., Dunne, E. M., Ehn, M., Gagné, S., Ickes, L., Junninen, H., Hansel, A., Kerminen, V.-M., Kirkby, J., Kupc, A., Laaksonen, A., Lehtipalo, K., Mathot, S., Onnela, A., Petäjä, T., Riccobono, F., Santos, F. D., Sipilä, M., Tomé, A., Tsagkogeorgas, G., Viisanen, Y., Wagner, P. E., Wimmer, D., Curtius, J., Donahue, N. M., Baltensperger, U., Kulmala, M., and Worsnop, D. R.: On the composition of ammonia-sulfuric acid clusters during aerosol particle formation, *Atmos. Chem. Phys. Discuss.*, 14, 13413–13464, doi:10.5194/acpd-14-13413-2014, 2014. 30802

Seinfeld, J. H. and Pankow, J. F.: Organic atmospheric particulate material, *Annu. Rev. Phys. Chem.*, 54, 121–140, doi:10.1146/annurev.physchem.54.011002.103756, 2003. 30802

Slemo, L.: The use of mass defect in modern mass spectrometry, *J. Mass Spectrom.*, 47, 226–236, doi:10.1002/jms.2953, 2012. 30806

Szmigielski, R., Surratt, J. D., Gómez-González, Y., Van der Veken, P., Kourtchev, I., Vermeylen, R., Blockhuys, F., Jaoui, M., Kleindienst, T. E., Lewandowski, M., Offenberg, J. H., Edney, E. O., Seinfeld, J. H., Maenhaut, W., and Claeys, M.: 3-methyl-1,2,3-butanetricarboxylic acid: An atmospheric tracer for terpene secondary organic aerosol, *Geophys. Res. Lett.*, 34, L24811, doi:10.1029/2007GL031338, 2007. 30803

Taatjes, C. A., Shallcross, D. E., and Percival, C. J.: Research frontiers in the chemistry of Criegee intermediates and tropospheric ozonolysis, *Phys. Chem. Chem. Phys.*, 16, 1704–1718, doi:10.1039/c3cp52842a, 2013. 30811

Taira, M. and Kanda, Y.: Continuous generation system for low-concentration gaseous nitrous acid, *Anal. Chem.*, 62, 630–633, doi:10.1021/ac00205a018, 1990. 30804

Tolocka, M. P., Jang, M., Ginter, J. M., Cox, F. J., Kamens, R. M., and Johnston, M. V.: Formation of oligomers in secondary organic aerosol, *Environ. Sci. Technol.*, 38, 1428–1434, doi:10.1021/es035030r, 2004. 30803

Title Page

Abstract

Introduction

Conclusions

References

Tables

Figures

◀

▶

◀

▶

Back

Close

Full Screen / Esc

Printer-friendly Version

Interactive Discussion



Vereecken, L. and Peeters, J.: Nontraditional (per)oxy ring-closure paths in the atmospheric oxidation of isoprene and monoterpenes, *J. Phys. Chem. A*, 108, 5197–5204, doi:10.1021/jp049219g, 2004. 30803

Vereecken, L., Harder, H., and Novelli, A.: The reaction of Criegee intermediates with NO, RO₂, and SO₂, and their fate in the atmosphere, *Phys. Chem. Chem. Phys.*, 14, 14682, doi:10.1039/c2cp42300f, 2012. 30811

Winkler, P. M., Ortega, J., Karl, T., Cappellin, L., Friedli, H. R., Barsanti, K., McMurry, P. H., and Smith, J. N.: Identification of the biogenic compounds responsible for size-dependent nanoparticle growth, *Geophys. Res. Lett.*, 39, L20815, doi:10.1029/2012GL053253, 2012. 30803

5

10

Discussion Paper | Discussion Paper

Discussion Paper | Discussion Paper

Discussion Paper | Discussion Paper

Composition and clustering of α -pinene oxidation products

A. P. Praplan et al.

[Title Page](#)

[Abstract](#)

[Introduction](#)

[Conclusions](#)

[References](#)

[Tables](#)

[Figures](#)

◀

▶

[Back](#)

[Close](#)

[Full Screen / Esc](#)

[Printer-friendly Version](#)

[Interactive Discussion](#)



Composition and clustering of α -pinene oxidation products

A. P. Praplan et al.

Table 1. Conditions of selected runs. The given values correspond to the period with constant $[H_2SO_4]$.

Run	α -pinene (pptv)	O ₃ (ppbv)	SO ₂ (ppbv)	HONO (ppbv)	H ₂ (%)	UV	[H ₂ SO ₄] cm ⁻³
1070.02	660	22	69	0	0.1	no	1.91×10^7
1100.02	1250	0.8	1.1	1.2–2.6	0	yes	1.03×10^7

[Title Page](#)[Abstract](#)[Introduction](#)[Conclusions](#)[References](#)[Tables](#)[Figures](#)[◀](#)[▶](#)[◀](#)[▶](#)[Back](#)[Close](#)[Full Screen / Esc](#)[Printer-friendly Version](#)[Interactive Discussion](#)

Composition and clustering of α -pinene oxidation products

A. P. Praplan et al.

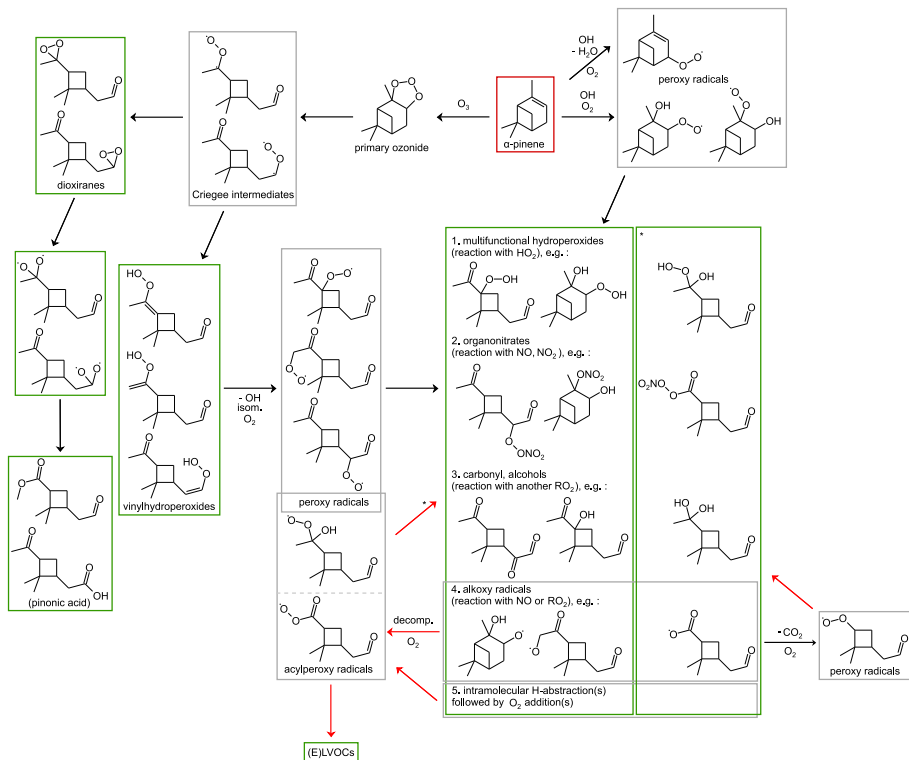


Figure 1. Non-exhaustive summary of α -pinene ozonolysis (left) and OH oxidation (right) reaction pathways. Not all possible reaction pathways and final products are displayed, but only representative examples. The box marked with a star (*) corresponds to products formed from (acyl)peroxy radicals via reactions 4 and 5. See main text and discussion for details.

Composition and clustering of α -pinene oxidation products

A. P. Praplan et al.

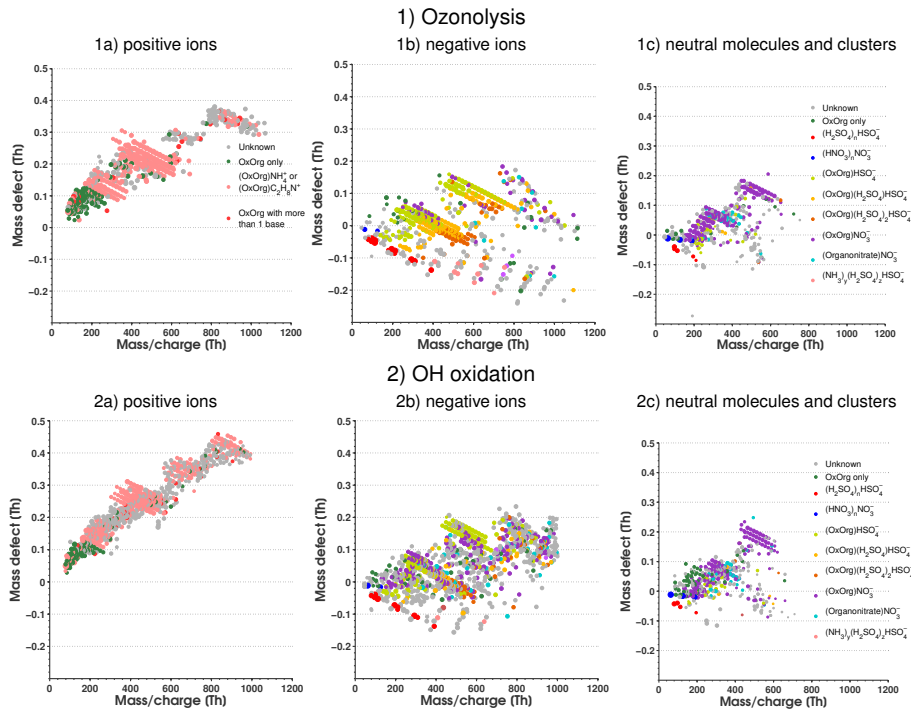


Figure 2. Mass defect plots derived from detected cations (positive API-TOF, left column), anions (negative API-TOF, middle column), and neutral molecular clusters (CI-API-TOF, right column) of α -pinene ozonolysis with OH scavenger (top row) and α -pinene oxidation by OH only (bottom row). The legend on the top left panel applies to the left column (positive clusters), while the legend on the top right panel applies to the middle and right columns (negative and neutral clusters).

Composition and clustering of α -pinene oxidation products

A. P. Praplan et al.

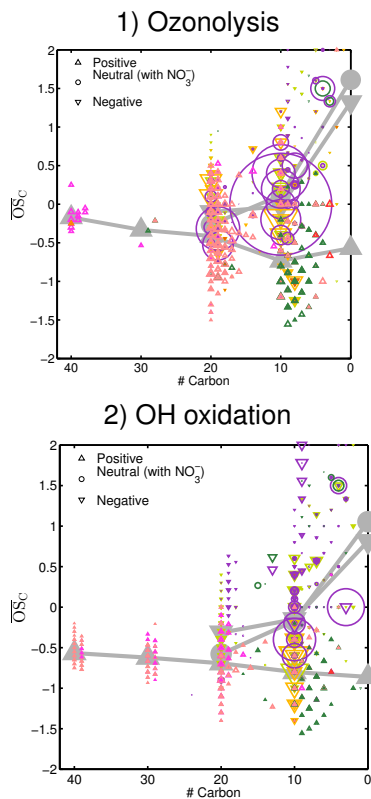


Figure 3. Mean carbon oxidation state (\overline{OS}_C) as a function of the number of carbons for each identified oxidised organic compound in clusters for all three instruments. The shape of the markers indicate which type of clusters is depicted and the colors are the same as in Fig. 2. The weighted mean for the various bands ($C < 8$, $C = 8–12$, $C = 18–20$, $C = 28–30$, and $C = 38–40$) is indicated with large gray symbols.

Composition and clustering of α -pinene oxidation products

A. P. Praplan et al.

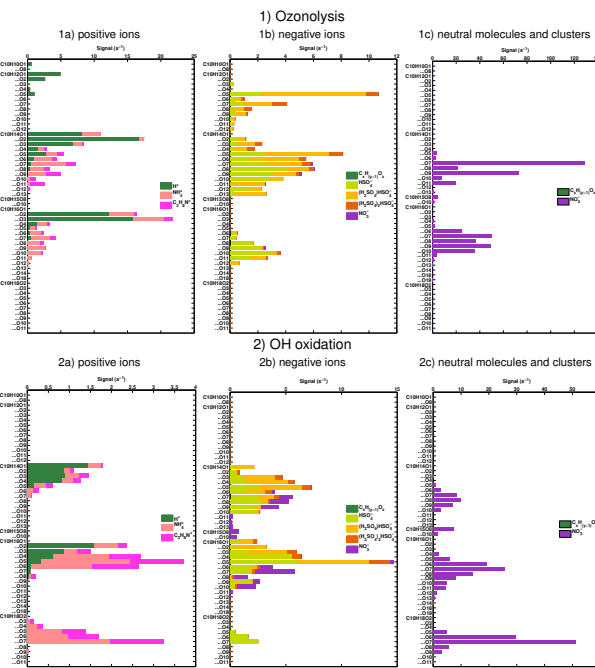


Figure 4. Stacked peak area for observed clusters containing $C_{10}H_bO_c$ according to core ion(s) of positive (left column), negative (middle column), and neutral (right column) clusters obtained from α -pinene ozonolysis with OH scavenger (top row) and α -pinene oxidation by OH only (bottom row).

Composition and clustering of α -pinene oxidation products

A. P. Praplan et al.

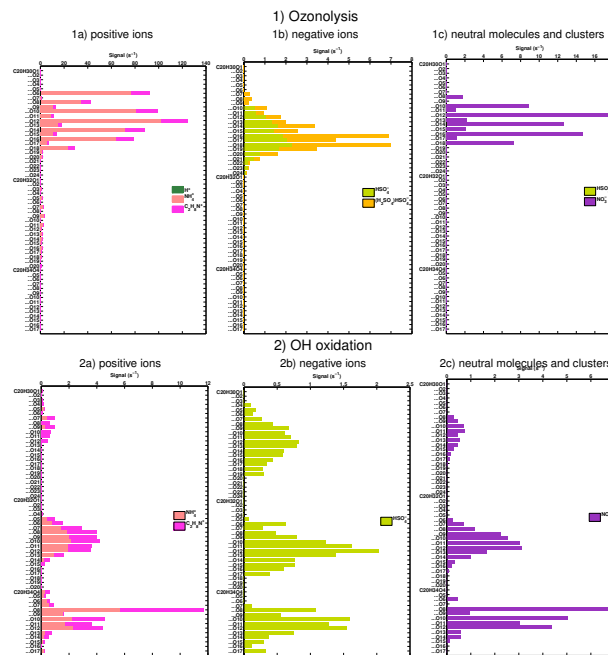


Figure 5. Stacked peak area for observed clusters containing $C_{20}H_bO_c$ according to core ion(s) of positive (left column), negative (middle column), and neutral (right column) clusters obtained from α -pinene ozonolysis with OH scavenger (top row) and α -pinene oxidation by OH only (bottom row).

Composition and clustering of α -pinene oxidation products

A. P. Praplan et al.

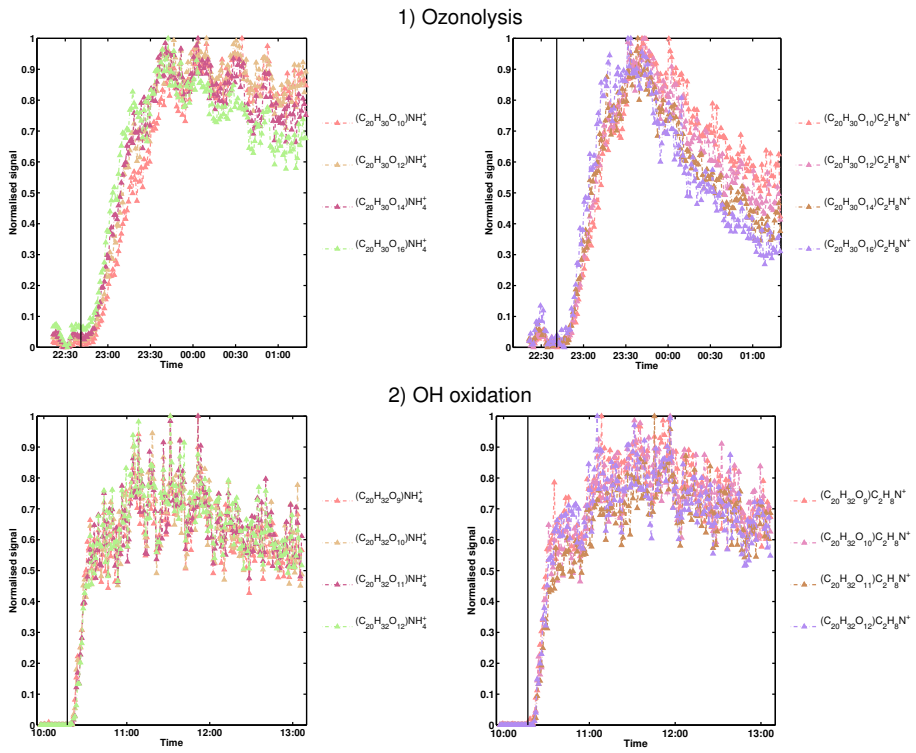


Figure 6. Time series of observed positive clusters containing $C_{20}H_{30,32}O_z$ oxidised compounds bound to NH_4^+ (left) and $C_2H_8N^+$ (right) for α -pinene pure ozonolysis (top row) and pure OH oxidation (bottom row). The vertical black line marks the beginning of the experiment.

Title Page

Abstract

Introduction

Conclusions

References

Tables

Figures



Back

Close

Full Screen / Esc

Printer-friendly Version

Interactive Discussion

Composition and clustering of α -pinene oxidation products

A. P. Praplan et al.

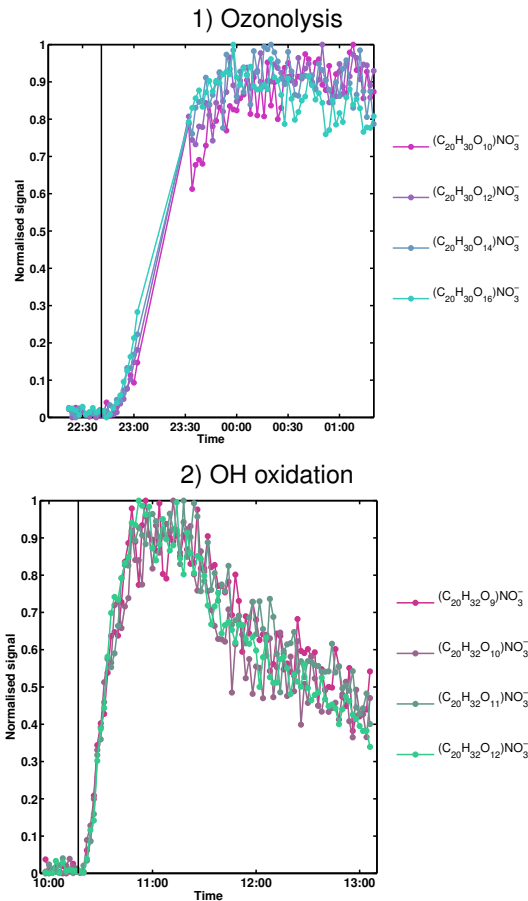


Figure 7. Time series of observed neutral clusters containing $C_{20}H_{30}O_z$ oxidised compounds for α -pinene pure ozonolysis (top row) and containing $C_{20}H_{32}O_z$ for pure OH oxidation (bottom row). The vertical black line marks the beginning of the experiment.

Composition and clustering of α -pinene oxidation products

A. P. Praplan et al.

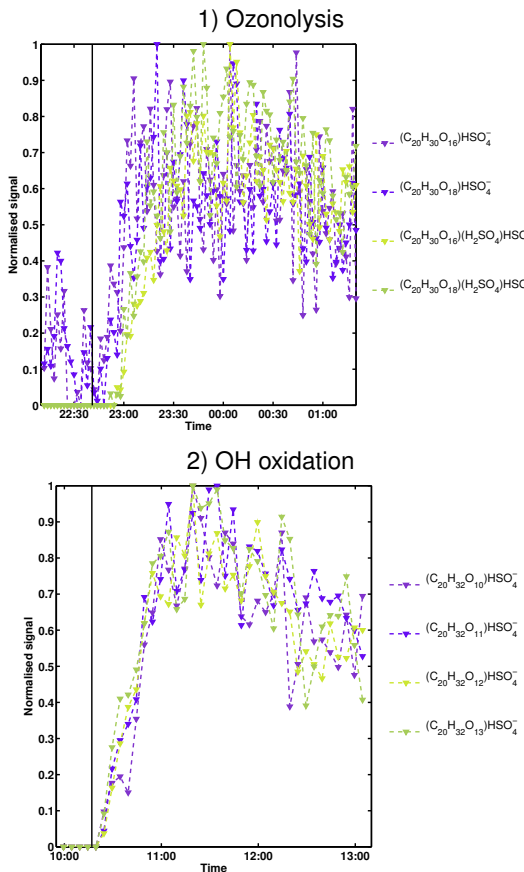


Figure 8. Time series of some observed negative clusters containing $C_{20}H_{30}O_z$ oxidised compounds for α -pinene pure ozonolysis (top row) and containing $C_{20}H_{32}O_z$ for pure OH oxidation (bottom row). The vertical black line marks the beginning of the experiment.